

University of Nebraska - Lincoln

DigitalCommons@University of Nebraska - Lincoln

Vadim Gladyshev Publications

Biochemistry, Department of

August 2006

Characterization of Alternative Cytosolic Forms and Cellular Targets of Mouse Mitochondrial Thioredoxin Reductase

Anton A. Turanov

University of Nebraska-Lincoln

Dan Su

University of Nebraska-Lincoln

Vadim N. Gladyshev

University of Nebraska-Lincoln, vgladyshev@rics.bwh.harvard.edu

Follow this and additional works at: <https://digitalcommons.unl.edu/biochemgladyshev>



Part of the [Biochemistry, Biophysics, and Structural Biology Commons](#)

Turanov, Anton A.; Su, Dan; and Gladyshev, Vadim N., "Characterization of Alternative Cytosolic Forms and Cellular Targets of Mouse Mitochondrial Thioredoxin Reductase" (2006). *Vadim Gladyshev Publications*. 63.

<https://digitalcommons.unl.edu/biochemgladyshev/63>

This Article is brought to you for free and open access by the Biochemistry, Department of at DigitalCommons@University of Nebraska - Lincoln. It has been accepted for inclusion in Vadim Gladyshev Publications by an authorized administrator of DigitalCommons@University of Nebraska - Lincoln.

Characterization of Alternative Cytosolic Forms and Cellular Targets of Mouse Mitochondrial Thioredoxin Reductase

Anton A. Turanov, Dan Su, and Vadim N. Gladyshev*

Department of Biochemistry, University of Nebraska–Lincoln, Lincoln, Nebraska 68588-0664

* Corresponding author — Dept. of Biochemistry, N151 Beadle Center, University of Nebraska–Lincoln, Lincoln, NE 68588-0664. Tel.: 402 472-4948; Fax: 402 472-7842; Email: vgladyshev1@unl.edu

Abstract: Thioredoxin reductase (TR) and thioredoxin (Trx) define a major cellular redox system that maintains cysteine residues in numerous proteins in the reduced state. Both cytosolic (TR1 and Trx1) and mitochondrial (TR3 and Trx2) enzymes are essential in mammals, but the function of the mitochondrial system is less understood. In this study, we characterized subcellular localization of three TR3 forms that are generated by alternative first exon splicing and that differ in their N-terminal sequences. Only one of these forms resides in mitochondria, whereas the two other isoforms are cytosolic. Consistent with this finding, TR3 did not have catalytic preferences for mitochondrial Trx2 versus cytosolic Trx1, both of which could serve as TR3 substrates. Similarly, TR1 was equally active with Trx1, Trx2, or a bacterial Trx. We generated recombinant selenoprotein forms of TR1 and TR3 and found that these enzymes were inhibited by zinc, but not by calcium or cobalt ions. We further developed a proteomic method for identification of targets of TRs in mammalian cells utilizing affinity columns containing recombinant TR3 forms differing in C-terminal sequences. Using this procedure, we found that Trx1 was the major target of TR3 in both rat and mouse liver cytosol. The truncated form of TR3 lacking selenocysteine was particularly efficient in binding Trx1, consistent with the previously observed role of truncated TR1 in apoptosis. Overall, these data establish that the function of TR3 is not limited to its role in Trx2 reduction.

Abbreviations: Trx, thioredoxin; TR, thioredoxin reductase; m, mouse; EGFP, enhanced green fluorescent protein; Sec, selenocysteine; SECIS, selenocysteine insertion sequence; h, human; r, rat; PBS, phosphate-buffered saline; DTT, dithiothreitol; EST, expressed sequence tag.

Introduction

The thioredoxin (Trx) system is one of the key cellular redox regulators (1). Together with the glutathione system, it controls the redox state of Cys residues in proteins and has numerous other roles in redox regulation of cellular processes. The Trx system is composed of thioredoxin reductase (TR) and Trx. TR is an FAD-containing pyridine nucleotide-disulfide oxidoreductase. It transfers electrons from NADPH to Trx, which in turn reduces thioredoxin peroxidase, methionine sulfoxide reductase, ribonucleotide reductase, and other redox proteins (2, 3).

Two Trx systems have been described previously in organisms

from yeast to mammals. One is present in the cytosol and is composed of TR1 (also called TXNRD1 or TrxR1) and Trx1 (4). The second is a mitochondrial system that consists of TR3 (also called TXNRD2 or TrxR2) and Trx2 (5, 6). In addition to the reduction of thioredoxins, TRs are capable of reducing a variety of cellular proteins and compounds (7, 8). Trx systems are present in all living organisms and are often required for viability. Cytosolic as well as mitochondrial Trx systems are essential for embryogenesis in mice, as deletion of any of their components (e.g. TR1, TR3, Trx1, or Trx2) has been reported to lead to embryonic lethality (9–12).

Both TR1 and TR3 occur in multiple forms generated by alternative splicing (13). There are at least six alternative TR1 forms that differ in their N-terminal residues, including one that contains an additional N-terminal glutaredoxin domain (14–16). Although alternative TR3 forms have been previously predicted (13, 17, 18), they have not been experimentally verified.

In this study, we describe the characterization of intracellular location of three alternative forms of TR3, two of which are extramitochondrial. Further characterization of kinetic parameters revealed that TR3 does not have a substrate preference for Trx2. Instead, we found that TR3 could efficiently interact with Trx1 and that Trx1 is a major TR3 substrate in the cytosol. Thus, the function of TR3 is not limited to its role in mitochondria.

Experimental Procedures

Materials—Dulbecco's modified Eagle's medium, fetal calf serum, and antibiotic/antimycotic mixture were from Invitrogen. EDTA, NADPH, sodium selenite, sodium phosphate, insulin, glycerol, Tris-HCl, HEPES, sucrose, NaCl, and *Escherichia coli* Trx were from Sigma. EDTA-free protease inhibitor mixture was from Roche Applied Science. LB medium and LB-agar medium powder were from Qbiogene, Inc. Horseradish peroxidase-coupled anti-rabbit and anti-mouse antibodies and ECL detection reagents were from Amersham Biosciences. Anti-human Trx1 monoclonal antibodies were purchased from Pharmingen, and anti-His tag antibodies from Invitrogen. Unless specified otherwise, all other reagents were from Sigma.

Construction of Mouse TR3, TR3a, TR3b, and TR3c Expression Vectors—Mouse (m) TR3 cDNA lacking sequences coding for the mitochondrial signal peptide was used as a cloning template, and mTR3a, mTR3b, and mTR3c cDNAs were amplified from it using *Pfu* Ultra polymerase (Stratagene) and the primers shown in the supplemental material. To prepare different mTR3-enhanced green fluo-

rescent protein (EGFP) fusion constructs, primer pairs 1, 3, 4, 5, and 6 (forward)/2 (reverse) were used to generate mTR3a-EGFP; primer pair 7/2 to generate mTR3b-EGFP; primer pairs 8/2 and 9/2 to generate mTR3c-EGFP; and primer pair 10/2 to generate mTR3 without EGFP (without the mitochondrial signal). The PCR products were cloned into the EcoRI and ApaI sites of pEGFP-N2 (Clontech). In all mTR3 constructs, the selenocysteine (Sec) codon (UGA) was mutated to a Cys codon (UGC). To generate constructs for overexpression of different mutant mTR3 proteins, the primers that are shown in the supplemental material were used. To prepare the mTR3 CU construct, primers 11/12 and 13 were used to generate an *E. coli fdhH* selenocysteine insertion sequence (SECIS) element downstream of the open reading frame. Primers 11/14 and 13 were used to prepare the mTR3 SU construct, which also contained the bacterial SECIS element. These sequences were inserted into pET-28a (Novagen) at NheI and EcoRI sites. The sequences of all constructs were verified by direct DNA sequencing at the Genomics Core Facility of the University of Nebraska.

Cell Culture, Transfection, and Subcellular Localization of mTR3 Isoforms—CV-1 cells were grown at 37 °C and 5% CO₂ in 25-cm² culture flasks in Dulbecco's modified Eagle's medium containing 1 mg/ml glucose and supplemented with 10% fetal calf serum. Transfections were carried out using Lipofectamine and PLUS reagent (Invitrogen). CV-1 cells were transfected with the constructs coding for different mTR3 isoforms fused to EGFP. The pEGFP-N2 vector was used as a control. Twenty-four hours after transfection, cells were washed with Opti-MEM I (Invitrogen) and subjected to staining. The cells were stained with MitoTracker, ER-Tracker, or LysoTracker (Molecular Probes) as recommended by the manufacturer. EGFP and Tracker fluorescence was visualized using Olympus FV500 inverted confocal microscopes at the Microscopy Core Facility of the University of Nebraska.

Overexpression of mTR3, Human (h) TR1, hTrx1, and Rat (r) Trx2 in E. coli—Bacterial expression constructs, including pET-28a-mTR3, pET-28a-hTR1, pET-15b-hTrx1, and pET-15b-rTrx2, were expressed in *E. coli* BL21(DE3) cells. The pET-15b-rTrx2 construct (kindly provided by Drs. Antonio Miranda-Vizuet and Giannis Spyrou) codes for rTrx2 that lacks the mitochondrial signal peptide. Cells were grown in LB medium containing kanamycin (50 µg/ml) or ampicillin (100 µg/ml) at 37 °C, and protein expression was induced with 0.5 mM isopropyl β-D-thiogalactopyranoside when cells reached ~0.6 *A*_{600 nm}. For expression of Sec-containing proteins, the pET-28a-mTR3-CU, pET-28a-mTR3-SU, and pET-28a-hTR1-CU constructs, containing an *E. coli fdhH* SECIS element, were used. These constructs were used alone, or the cells were cotransformed with the pSUABC plasmid (kindly provided by Dr. Elias Arnér). pSUABC contains chromosomal fragments containing *E. coli selA*, *selB*, and *selC* genes under the control of their endogenous promoters. Protein expression was induced by addition of 0.5 mM isopropyl β-D-thiogalactopyranoside when cells reached ~0.6 *A*_{600 nm}. Sodium selenite was added 1 h prior to induction to a final concentration of 2 µM. After the induction, cells were grown overnight at 30 °C, harvested by centrifugation, and stored at –80 °C until used.

Purification of Recombinant Proteins—*E. coli* cells were resuspended at 4 °C in 50 mM sodium phosphate and 150 mM NaCl (pH 8.0) containing EDTA-free protease inhibitor mixture and sonicated. Following centrifugation at 14,000 rpm for 30 min at 4 °C, the supernatant fraction was loaded onto a 10-ml TALON™ column (Clontech). Recombinant proteins containing N-terminal His tags were eluted with a linear gradient of 20–200 mM imidazole in loading buffer. Fractions containing hTrx1 or rTrx2 were pooled, dialyzed

against phosphate-buffered saline (PBS), and stored at –80 °C. Fractions containing mTR3 or hTR1 were pooled, dialyzed against PBS (pH 7.3), and applied to a 5-ml 2',5'-ADP-Sepharose column (Amersham Biosciences) equilibrated with PBS. The bound proteins were eluted with 1 M NaCl in PBS, and fractions containing pure proteins were dialyzed against PBS and stored at –80 °C. The N-terminal His tags were removed using a His tag cleavage kit (Novagen).

Antibodies and Western Blot Analyses—Polyclonal antisera against mTR3 and hTR1 were produced by immunization of rabbits with recombinant mTR3 and hTR1 proteins that contained Cys in place of Sec. Polyclonal antisera against hTrx1 and rTrx2 were produced by immunization of rabbits with recombinant full-length hTrx1 and an rTrx2 form lacking the mitochondrial signal peptide. SDS-PAGE analyses were carried out using NuPAGE Novex gels (Invitrogen), followed by transfer of proteins onto polyvinylidene difluoride membranes. In Western blot assays, antisera were used at the following dilutions: 1:4000 for TR3, 1:2000 for TR1, 1:2000 for Trx2 and Trx1, and according to the manufacturer's instructions for hTrx1 and proteins containing His tags. Immunoblot signals were visualized using an ECL detection system (Amersham Biosciences).

Thioredoxin Reductase Assay—The concentration of TRs was determined by measuring the flavin absorbance at 460 nm (molar extinction coefficient of 11.3 mM⁻¹ cm⁻¹) or the absorbance at 280 nm and subtracting the absorbance at 310 nm (molar extinction coefficient of 65 mM⁻¹ cm⁻¹). For other purposes, the protein concentration was determined using the Bradford assay (Bio-Rad). TR and Trx activities were determined using the insulin reduction assay as described previously (19). Reaction mixtures (500 µl) containing 3 µM TR3 or TR1 were used. The reaction was followed by a decrease in absorbance at 340 nm resulting from oxidation of NADPH. Apparent *K*_m values were calculated from Lineweaver-Burk plots of 1/*v* versus 1/[S]. A molar extinction coefficient of 6220 M⁻¹ cm⁻¹ was used to calculate the *k*_{cat} value. To test for inhibition of TR activity by metals, the proteins were incubated with the indicated concentrations of metal ions (Ca²⁺, Zn²⁺, and Co²⁺) for 5–10 min prior to adding them to the reaction mixtures. To study the role of EDTA, the reactions were carried out in the presence of the indicated concentrations of EDTA.

Cell Fractionation—Cell fractionation was carried out by differential centrifugation. Briefly, rat livers (10–20 g) or mouse livers (2–5 g) were washed twice with ice-cold PBS and lysed on ice by 60 Dounce strokes with a tight fitting pestle in buffered sucrose containing 20 mM HEPES (pH 7.5), 250 mM sucrose, 1 mM EDTA, 1 mM EGTA, 10 mM KCl, and Complete protease inhibitor mixture (one tablet/10 ml; Roche Applied Science). After two centrifugation runs at 1000 × *g* to discard nuclei, mitochondria were pelleted at 10,000 × *g*, washed once, resuspended in buffered sucrose, and stored at –80 °C. The cytosolic fraction was obtained by centrifugation of the post-mitochondrial supernatant at 100,000 × *g* for 1 h. To obtain mitochondrial lysate, an aliquot of the mitochondrial fraction was thawed, resuspended in an appropriate buffer, and sonicated, and the mitochondrial lysate was collected by centrifugation at 10,000 × *g*. The protein content was determined by the Bradford assay.

Preparation of mTR3-immobilized Resins and Target Search—TR3-immobilized resins were prepared using a previously described procedure for preparing Sepharose-based affinity columns (20). Briefly, mutant mTR3 proteins in 100 mM sodium carbonate buffer (pH 9.5) containing 0.5 M NaCl were incubated with cyanogen bromide-activated Sepharose 4B (Sigma) that had been swelled in the same solution for 2 h at room temperature according to the manufacturer's instructions. The coupling reaction was stopped by centrifugation, and

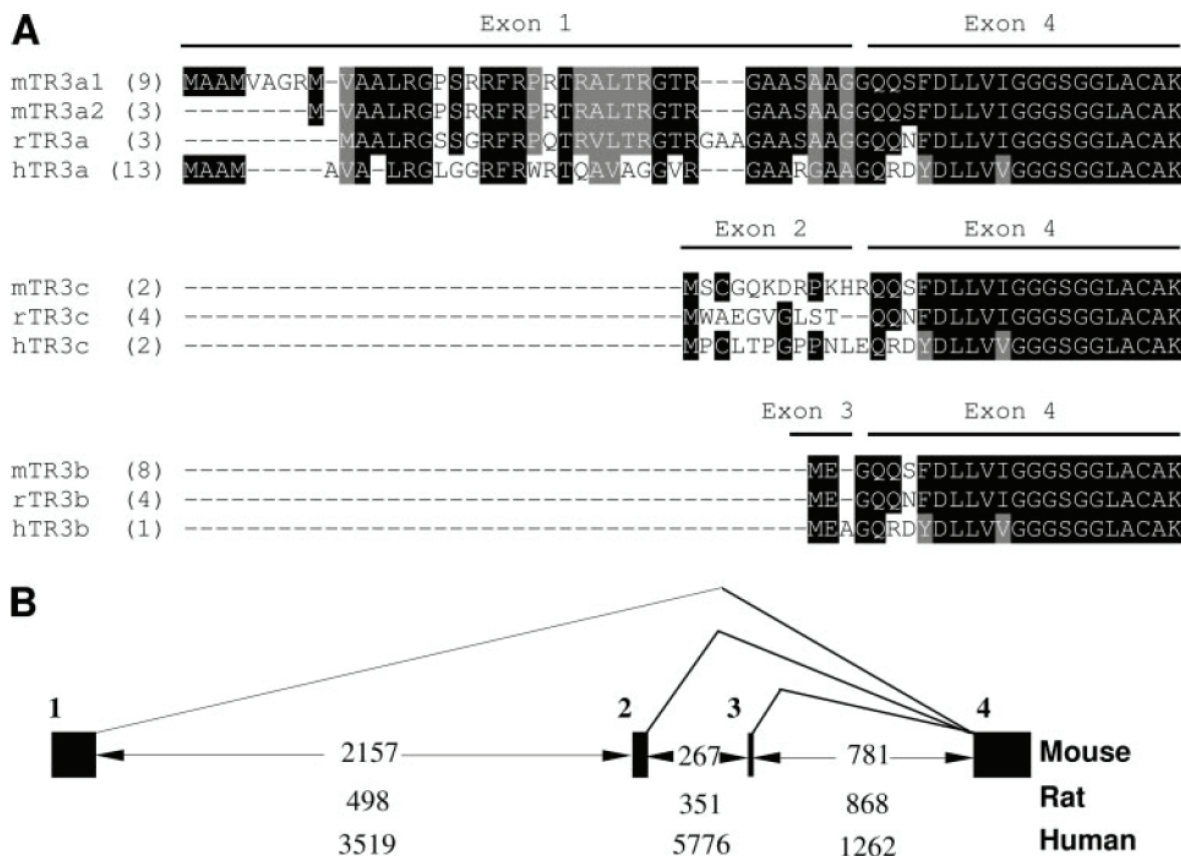


FIGURE 1. Alternative forms of mammalian TR3. *A*, amino acid sequence comparison of TR3 isoforms. The N-terminal regions of different alternative forms of mouse, rat, and human TR3 are shown. The numbers in parentheses indicate the numbers of corresponding ESTs that were found in data bases. Identical residues within each of the three groups of sequences are highlighted. *B*, structural organization of mouse, rat, and human TR3 genes. Each numbered box represents an exon within the gene. (Only the first four exons are shown.) There are three alternative forms of mTR3 mRNA that are differentially encoded by exons 1–3, followed by the common exon 4. The numbers between boxes indicate the lengths of introns (in base pairs) in the indicated genomes.

unreacted side chains on the resin were blocked by incubation with 50 mM Tris-HCl (pH 8.0) for 12 h at 4 °C. Immobilized TR3 was quantified based on the difference between the amounts of TR3 initially used and remaining in solution after the coupling reaction. Typically, >80% of the proteins could be immobilized. To search for TR3 targets, rat or mouse liver mitochondrial or cytosolic lysates (10 mg of protein) were incubated with 0.5 ml of mTR3-immobilized resin containing 5 mg of TR3 at 25 °C for 1 h under gentle stirring. Immobilized TR3 was initially reduced with 0.2 mM NADPH for 30 min. The resins were washed with 50 mM Tris-HCl (pH 8.0) and 200 mM NaCl to remove nonspecifically bound proteins. The washing was repeated until the absorbance of the wash fraction at 280 nm was negligible. Finally, the resin was suspended in 50 mM Tris-HCl (pH 8.0), 200 mM NaCl, and 10 mM dithiothreitol (DTT) or 0.2 mM NADPH and incubated for 30 min at 25 °C. Eluted proteins were separated from the resin by centrifugation and collection of the soluble fractions. The proteins were fractionated on SDS-polyacrylamide gels and visualized by Western blot analyses or subjected to staining with a Bio-Safe Coomassie or silver staining kit (Bio-Rad) and identification of the proteins by tandem mass spectrometry at the Mass Spectrometry Facility of the University of Nebraska.

Results

Identification and Subcellular Localization of TR3 Isoforms Generated by Alternative First Exon Splicing—By exhaustive searches

of non-redundant and expressed sequence tag (EST) data bases, we detected several cDNA forms of mTR3, each represented by multiple ESTs. These forms differed in their 5'-sequences followed by common sequences corresponding to the core part of TR3, indicating alternative first exon splicing (Figure 1). In addition to the mouse sequences, the corresponding forms were found in human and rat sequences, suggesting conservation of alternative splicing to generate multiple forms of TR3 in mammals. All detected TR3 cDNAs could be organized into three groups that resulted in unique open reading frames differing in their N-terminal sequences (Figure 1*A*). The first form (TR3a) contains a predicted N-terminal signal peptide for mitochondrial targeting. It is represented by 12 ESTs in mice, 3 in rats, 13 in humans, and 1 in dog (GenBank™ accession number DN387361 [GenBank]). Three mTR3 ESTs were slightly shorter than the remaining nine sequences containing the predicted translation initiation codon. However, two additional candidate initiation codons were found immediately downstream. Initiation of translation from any of the three codons was predicted to produce a mitochondrial form of the enzyme. The shorter form was designated as mTR3a2. Analysis of the Kozak consensus requirements (GCCRCCAUGG, where R = A or G) for translation initiation revealed that both the first (CGGACCAUGG) and third (GCGGCGAUGG) AUG codons have favorable consensus sequences and can initiate translation of mitochondrial mTR3. Thus, the mTR3a1 isoform is likely the major mitochondrial TR3 isoform in mice.

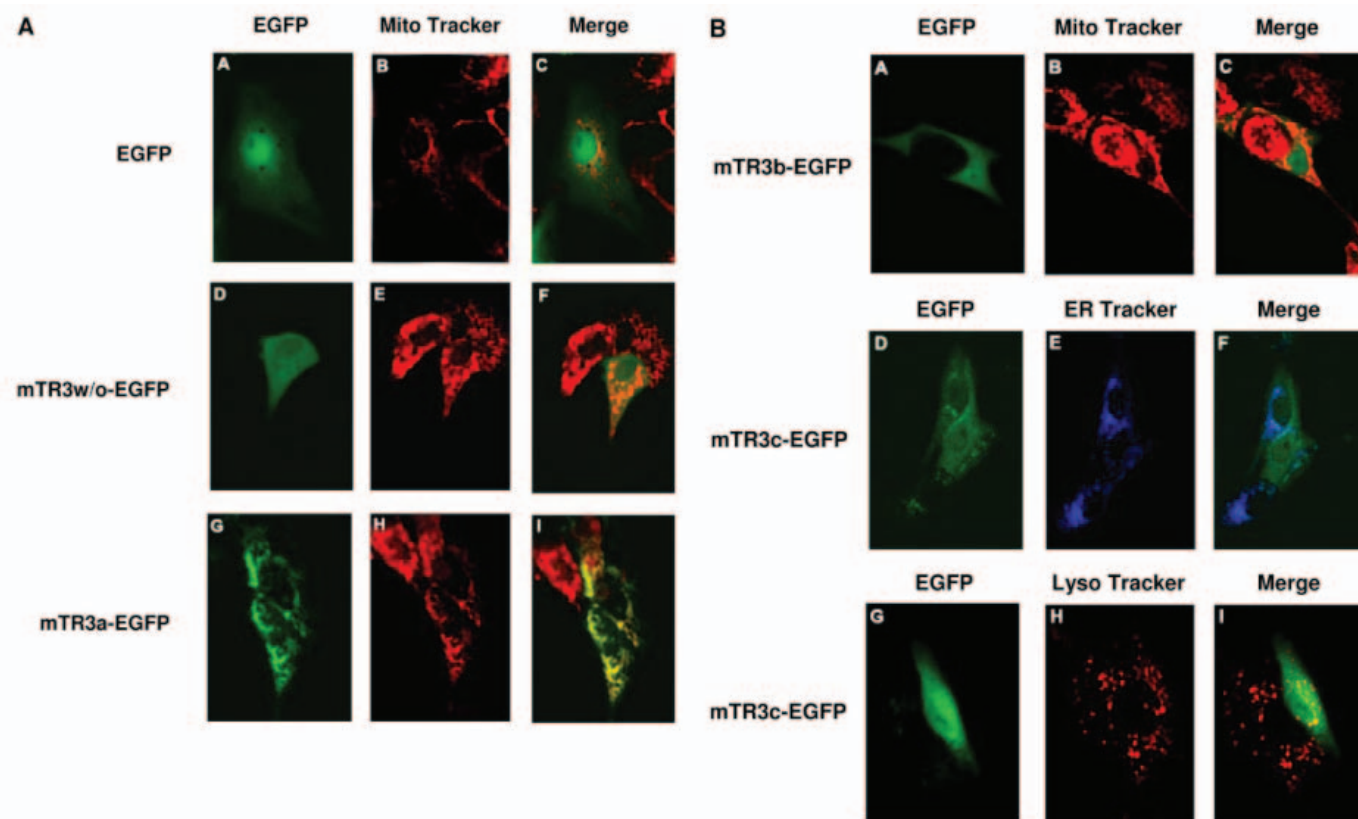


FIGURE 2. Subcellular localization of alternatively spliced forms of mTR3. CV-1 cells were transfected with indicated constructs coding for various TR3-EGFP fusion proteins, and the cells were analyzed for EGFP fluorescence by confocal microscopy. To identify the location of TR3 fusion proteins, cells were co-stained with organelle-specific fluorescent dyes (MitoTracker, ER-Tracker, and LysoTracker). *A*, localization of mTR3a. *Panels A, D, and G*, detection of TR3-EGFP fusion proteins by EGFP fluorescence; *panels B, E, and H*, staining with MitoTracker Red; *panels C, F, and I*, merged images of MitoTracker and EGFP signals. *B*, localization of the mTR3b and mTR3c isoforms. *Panels A, D, and G*, detection of TR3-EGFP fusion proteins by EGFP fluorescence; *panels B, E, and H*, mitochondrial staining with MitoTracker Red; *panel E*, endoplasmic reticulum staining with ER-Tracker Blue; *panel H*, lysosome staining with LysoTracker Red; *panels C, F, and I*, merged images of the indicated organelle Trackers and EGFP signals.

Two other forms (TR3b and TR3c) have shorter predicted N-terminal sequences and lack predicted signal sequences. TR3b is represented by eight ESTs in mouse (GenBank™ accession numbers CN664710 [GenBank], BY226497 [GenBank], BB843112 [GenBank], BB842317 [GenBank], BY128436 [GenBank], BY217359 [GenBank], BY211475 [GenBank], and BB566223 [GenBank]), four ESTs in rat (accession numbers CV114471 [GenBank], CB757630 [GenBank], CB708769 [GenBank], and CK482696 [GenBank]), and one EST in human (accession number DN998641 [GenBank]). This form was previously predicted, but not characterized (13). TR3c is represented by two ESTs in mouse (accession numbers BY707998 [GenBank] and AK008004 [GenBank]), four ESTs in rat (accession numbers AI555332 [GenBank], CO393277 [GenBank], CK468797 [GenBank], and CB759068 [GenBank]), and two ESTs in human (accession numbers BX489630 [GenBank] and BE146928 [GenBank]). It has not been described previously. The three forms utilize alternative first exons 1–3, followed by common exon 4 (Figure 1*B*). Similar gene architectures are used to generate alternative TR3 forms in mouse, rat, and human genomes (Figure 1*B*). The order of exons is also conserved, although intron sequences are longer in humans compared with rodents.

The cDNAs for TR3b and TR3c were cloned in the pEGFP-N2 expression vector to generate fusion proteins containing C-terminal EGFP. We also cloned the TR3a cDNA with and without the mitochondrial signal peptide. To increase the expression level of proteins,

the C-terminal penultimate Sec codon was replaced with a Cys codon in all constructs. The four constructs were then used to assess subcellular localization of the three TR3 forms in CV-1 cells (Figure 2). Consistent with the previous data for the mitochondrial form of TR3, the TR3a-EGFP protein was targeted to mitochondria (Figure 2*A*, *panels G–I*). However, in the absence of the mitochondrial signal peptide, the protein was detected in the cytosol (Figure 2*A*, *panels D–F*). The TR3b form has only a three-amino acid (in mice and rats) or four-amino acid (in humans) extension over the common sequence derived from exon 4. The protein with this short extension was cytosolic. The TR3c form has a 12-amino acid (in mice and humans) or 10-amino acid (in rats) extension and had a cytosolic location, but the signal exhibited a non-uniform distribution. The regions enriched in TR3c corresponded to neither the endoplasmic reticulum nor lysosomes (Figure 2*B*, *panels D–I*). Overall, these data show that the location of TR3 is not limited to mitochondria and that at least two additional extramitochondrial forms exist. All TR3 forms appear to have unique cellular distribution properties.

Preparation and Characterization of Sec-containing Recombinant mTR3 and hTR1—Sec-containing TR1 was previously expressed in *E. coli* from a construct in which a SECIS element derived from the *E. coli fdhH* gene was placed downstream of the TR1 open reading frame (16, 21–23). To express Sec-containing TR3, we cloned mTR3 cDNA (without the sequence coding for the mitochondrial signal peptide) followed by the *fdhH* SECIS element into the

pET-28a(+) vector. Recombinant His-tagged TR3 was isolated by affinity chromatography on TALON resin. Sec insertion is known to be inefficient during expression of recombinant selenoproteins. We estimated the amount of selenium in the TR3 preparation by inductively coupled plasma mass spectrometry and found that only 5% of the protein was in the Sec-containing form. To increase the yield of the Sec-containing protein, we coexpressed the TR3 construct with the *E. coli selA*, *selB*, and *selC* genes, which code for Sec synthase, Sec-specific elongation factor, and tRNA^{Sec}, respectively (21, 24). In the case of TR3, this procedure allowed a dramatic increase in the efficiency of Sec insertion, as the new TR3 preparation had ~0.5 eq of selenium, suggesting that 50% of the enzyme molecules were in the Sec-containing form. We repeated this experiment several times and found that the Sec-containing protein accounted for 41–65% of the recombinant enzyme preparations. We similarly cloned and prepared His-tagged Sec-containing hTR1, which also contained ~0.5 eq of selenium when coexpressed with *selA*, *selB*, and *selC*.

To our knowledge, TR3 has not been previously assayed as reductant for mammalian mitochondrial Trx2, its predicted natural substrate. In addition, no comparative analyses have previously been performed for TR1 and TR3. We characterized the catalytic properties of recombinant TR3 and TR1 using a spectrophotometric assay of Trx-dependent insulin reduction (19). We used three different recombinant thioredoxins as substrates for these enzymes, including hTrx1, rTrx2 and *E. coli* Trx. Because TR3 and Trx2 are known as mitochondrial proteins and TR1 and Trx1 as cytosolic proteins, the expectation was that these protein pairs may show the best kinetic parameters. However, we found that the TR3/Trx2 pair had the highest K_m and the lowest catalytic efficiency of all tested enzyme-substrate combinations (Table 1). In addition, *E. coli* Trx was the best substrate for both mammalian TRs. Nevertheless, the differences in kinetic parameters were not dramatic, and the overall data suggest that the efficiency of TR1-based Trx reduction is nearly equal for Trx1 and Trx2 and that TR3 can reduce Trx1 and Trx2 with similar catalytic efficiency. These data are consistent with the results of TR3 intracellular localization experiments. Because the protein is located in different cellular compartments, it may be able to efficiently reduce various thioredoxins, not just the one in mitochondria.

Inhibition of Thioredoxin Reductase Activity by Metal Ions—

It was previously observed that EDTA is required for TR1 catalytic activity, presumably because of inhibition of the enzyme by heavy metal ions present in the reaction mixture (19). In addition, a previous study suggested that Ca²⁺ might be a potential inhibitor of mamma-

lian TR (25–27), although another study found no inhibitory effects of calcium on TR1 activity (28). The possibility remained that the differences observed were due to analyses of different TR isozymes.

We tested various metal ions for their effect on the catalytic activities of recombinant TR1 and TR3 in *in vitro* assays of insulin reduction using *E. coli* Trx as a substrate. The presence of EDTA was required for the activities of both TR1 and TR3 (Figure 3), and progressive increases in the EDTA concentration increased the activities of both enzymes. If the concentration of EDTA in the reaction mixture was higher than 100 μM (up to 1 mM tested) (data not shown), the enzymes were fully active.

We next tested the effect of Ca²⁺ on TR1 and TR3 activities and further extended these studies to include Zn²⁺ (Figure 4). In this experiment, TR1 and TR3 were preincubated for 5 min with different concentrations of metal ions prior to adding the enzymes to reaction mixtures containing 100 μM EDTA. The data clearly indicated that addition of Ca²⁺ ions had no effect on either TR1 or TR3 activity up to concentrations higher than the physiological levels (up to 5 mM). In contrast, Zn²⁺ completely inhibited both enzymes at 100–200 μM and above. Above 200 μM Zn²⁺ for TR1 and 300 μM Zn²⁺ for TR3, enzymes precipitated, which precluded activity assays at high concentrations of this metal ion.

In the experiments described above, the recombinant TR1 and TR3 we used had N-terminal His tags and were purified by metal affinity chromatography on a TALON resin. Because this resin contains chelated Co²⁺ ions, the possibility remained that these ions contaminated the protein preparations, thereby inhibiting enzyme activities. To test this possibility, we determined the influence of Co²⁺ on TR1 and TR3 activities (Figure 5) and found that this metal ion had no significant inhibitory effect, although some inhibition was observed at higher concentrations of Co²⁺.

TABLE 1. Kinetic parameters for hTR1 and mTR3

Substrate	K_m μM	k_{cat} min ⁻¹	k_{cat}/K_m
hTR1			
<i>E. coli</i> Trx	1.57	2794	1180
Human Trx1	1.83	1547	845
Rat Trx2	1.41	1644	1118
mTR3			
<i>E. coli</i> Trx	2.56	1770	691
Human Trx1	2.36	1198	508
Rat Trx2	5.1	2273	446

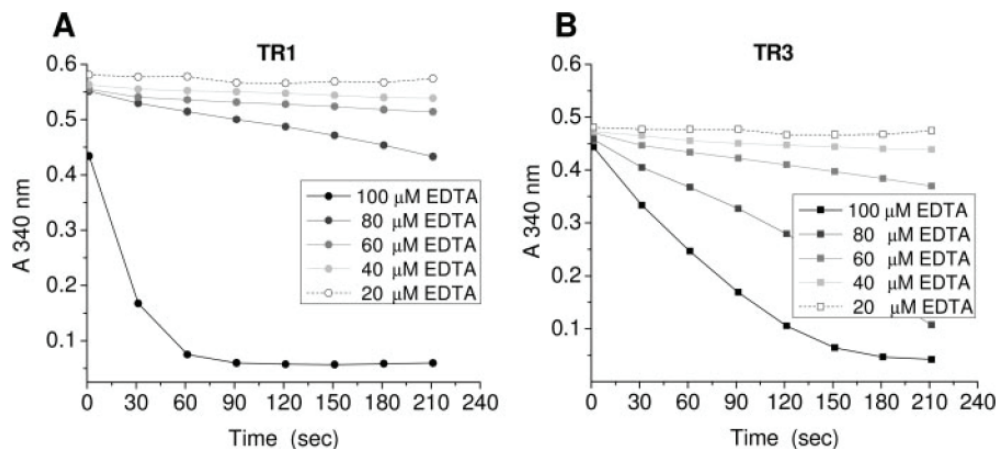


FIGURE 3. Effect of EDTA on TR1 and TR3 activities. TR activity was assayed by following NADPH oxidation in a Trx-dependent reduction of insulin. The indicated concentrations of EDTA (20–100 μM) were used in the reaction mixtures. A, TR1 activity; B, TR3 activity.

To further test a possible role of the His tag as a metal chelator, we removed this tag from both enzymes by proteolysis with thrombin. We also dialyzed the substrate (*E. coli* Trx) overnight against PBS containing 1 mM EDTA. Again, we found that zinc inhibited TR1 and TR3 activities (Figure 6). This inhibitory effect might be explained by high natural affinity of Zn^{2+} for dithiols. Mammalian TRs have two such pairs: the CXXXXC motif in the N-terminal active site and the CU motif (where U is selenocysteine) at the C terminus. Zn^{2+} presumably binds to one or both of these essential sites and completely inhibits the enzymes.

Identification of TR3 Target Proteins—The presence of TR3 in different cellular compartments implies that it may have multiple substrates. To identify protein targets of TR3, we prepared various mutant forms of this protein and used them as affinity matrices. The following TR3 forms were prepared: (i) wild-type TR3 containing a C-terminal GCUG tetrapeptide (this sample was a 1:1 mix-

ture of the Sec-containing form and the form truncated at the Sec UGA codon), (ii) a mutant in which Cys in the C-terminal tetrapeptide was replaced with Ser (GSUG) (this form also was a 1:1 mixture of the Sec-containing form and the form truncated at Ser), (iii) a mutant in which Sec was replaced with Cys (GCCG), (iv) a mutant in which Sec in the C-terminal tetrapeptide was replaced with Cys and Cys was replaced with Ser (GSCG), (v) a mutant in which both Cys and Sec were replaced with Ser residues (GSSG), and (vi) a truncation mutant in which the Sec codon functioned as a stop codon (GC-stop) (Table 2). Each TR3 form was then linked to cyanogen bromide-activated Sepharose to prepare mTR3-immobilized affinity resins. We hypothesized that, by using these affinity matrices, the target proteins in cell lysates could be enriched through formation of mixed disulfide or selenenylsulfide intermediates with immobilized TR3. A schematic representation of our method is shown in Figure 7.

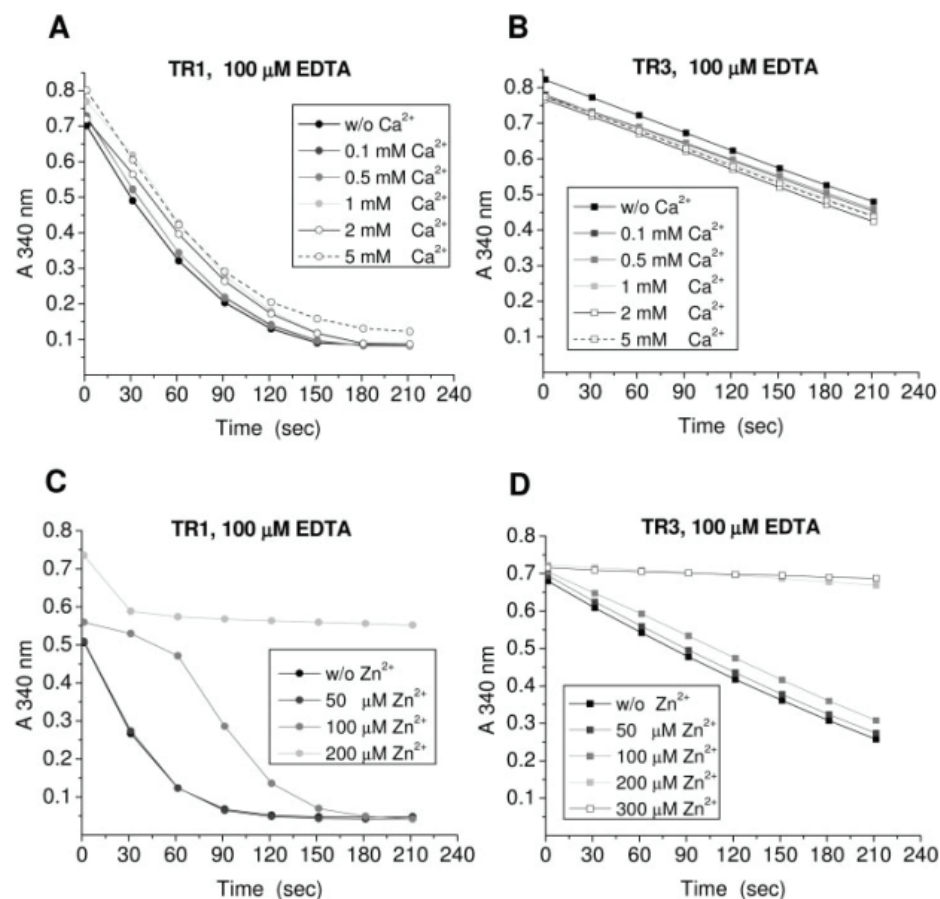


FIGURE 4. Effects of Ca^{2+} and Zn^{2+} ions on TR1 and TR3 activities. TR activities were assayed as Trx-dependent reduction of insulin. TR1 and TR3 were first preincubated with the indicated concentrations of metal ions (Ca^{2+} (A and B) and Zn^{2+} (C and D)) for 5 min, followed by addition of the enzymes to the reaction mixture.

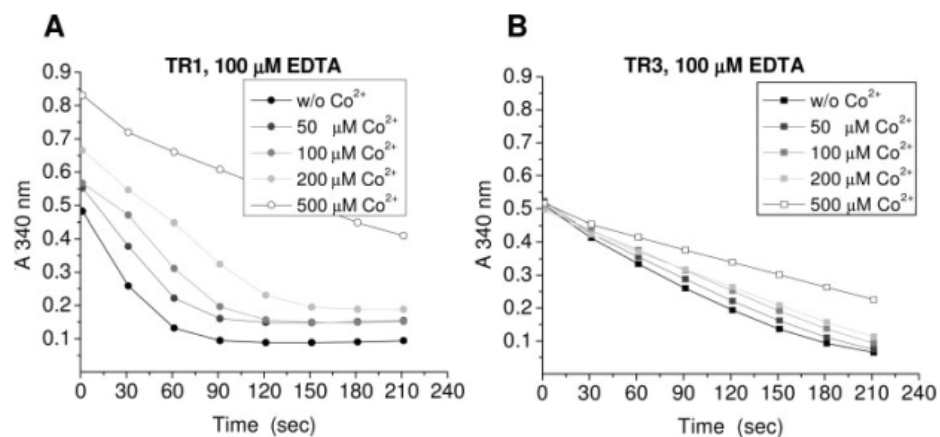


FIGURE 5. Effect of Co^{2+} ions on TR1 and TR3 activities. Trx-dependent insulin reduction was used to assay TR activities. TR1 and TR3 were preincubated with the indicated concentrations of Co^{2+} for 5 min, followed by addition of the enzymes to the reaction mixtures. A, TR1 activity; B, TR3 activity.

It was previously proposed that Sec is essential for catalysis by mammalian TRs (29, 30). Sec is thought to act as an attacking group and to reduce the active-site disulfide in oxidized thioredoxins, forming an intermediate selenenylsulfide bond between TR and the Trx substrate, whereas the Cys adjacent to Sec is thought to act as a resolving residue, which reduces the selenenylsulfide. Alternatively, the Cys might be the residue attacking the substrate, and Sec may serve as the resolving residue. If this is the case, one would expect to find differences in the ability of mutant TR3 forms to bind target proteins. In particular, GSUG, GC, and GSCG mutants would be expected to stabilize the mixed selenenylsulfide or disulfide bonds between TR3 and thioredoxin or others targets, whereas GCUG, GCCG, and especially GSSG mutants would be expected to either complete the reaction or not interact with the substrate.

To identify cellular targets, the immobilized mTR3 forms were reduced with NADPH and briefly washed with a buffer to remove the excess reductant, and rat liver mitochondrial or cytosolic lysates were added to each resin. Following incubation and washing, the target proteins were eluted by adding a DTT-containing buffer (Figure 8). Analysis of Coomassie Blue-stained gels revealed several protein bands that were present independently of the TR3 form used. Therefore, the binding of these proteins either was nonspecific or did not involve the C-terminal tetrapeptide, suggesting that most of these proteins are not specific redox-active TR3 substrates. It is possible that some of these weakly bound proteins are regulators of TR3 function or can be regulated by TR3 independent of the redox function.

Among the detected proteins, one prominent band had an approximate molecular mass of 12 kDa. Migration of this band on SDS-polyacrylamide gels corresponded to the predicted mass of thioredoxin, the substrate of TR3. It was particularly abundant in the cytosolic fraction, but was also detected in the mitochondrial fraction. Tandem mass spectrometric sequencing of the 12-kDa protein eluted from various TR3 resins and in both the cytosolic and mitochondrial fractions identified this protein as Trx1. Interestingly, we did not detect peptides derived from Trx2 in either the mitochondrial or cytosolic fractions eluted from the TR3 columns. The trace amount of cytosolic Trx1 in the mitochondrial fraction could probably be explained as cytosolic contamination of the mitochondrial fraction. Thus, Trx1 was specifically enriched on the TR3 affinity columns.

To decrease the nonspecific binding of cellular proteins to the mTR3-immobilized resins, we extended the washing procedure and increased the ionic strength of the wash buffer. This procedure decreased the binding of many proteins to the resin; however, the 12-kDa band remained the major protein bound to TR3 in the cytosolic fraction (in two samples) and was also detected as the protein enriched in the mitochondrial fractions (Figure 9). The 12-kDa bands

were again subjected to sequencing and found to contain exclusively Trx1. It should be stressed that the TR3-C form (truncated TR3) was particularly efficient in binding Trx1. This form is thought to exist *in vivo* because of truncation of TR synthesis at the UGA codon. Moreover, truncated TR1 was found to cause apoptosis in mammalian cells (31), although the mechanism of this effect is not known. Our finding provides a possible explanation of this effect, suggesting that apoptosis is promoted by the formation of stable complexes between truncated TRs and thioredoxins, inactivating both molecules and disrupting redox homeostasis.

To further examine the specificity of interactions between TR3 and target proteins in rat liver samples, we extended the studies to mouse liver mitochondrial and cytosolic fractions. A strong band was detected at ~12 kDa in the mouse liver cytosolic samples eluted from TR3-CU, TR3-SC, and TR3-C (but not TR3-SS) affinity columns (data not shown). We also detected a weak 12-kDa band in the mouse liver mitochondrial samples. As in the cytosolic fractions, this protein band was enriched in the samples eluted from TR3-CU, TR3-SC, and TR3-C columns, but was not detected in the sample eluted from the TR3-SS resin. Thus, these results are consistent with those from the rat liver experiments.

The mouse and rat fractions eluted from the affinity columns were further subjected to Western blotting with anti-Trx1 and anti-Trx2 polyclonal antisera. Using anti-Trx1 antibodies, we found that Trx1 was specifically bound and eluted by DTT from the resins, confirming the tandem mass spectrometric data. Also consistent with the mass spectrometry data, rat and mouse cytosolic Trx1 specifically interacted with TR3-CU, TR3-SU, TR3-CC, TR3-SC, and TR3-C resins and did not bind TR3-SS (Figure 10, B and D).

In the case of Trx2 and mitochondrial samples, we detected bands corresponding to the molecular mass of Trx2, which were eluted from TR3-SC and TR-C columns (Figure 10, A and C). Co-migration of these bands and the control Trx2 bands detected with anti-Trx2 antibodies in the original cytosolic and mitochondrial fractions supported their assignment as Trx bands. Unexpectedly, enrichment of Trx2 was poor on the TR3 columns, especially compared with that of Trx1, indicating that only a small fraction of Trx2 was bound to the

TABLE 2. C-terminal mutant mTR3 proteins

C-terminal tetrapeptide	SECIS	Abbreviation
Gly_Cys_Sec_Gly	<i>E. coli fdhH</i>	CU
Gly_Ser_Sec_Gly	<i>E. coli fdhH</i>	SU
Gly_Cys_Cys_Gly		CC
Gly_Ser_Cys_Gly		SC
Gly_Ser_Ser_Gly		SS
Gly_Cys_		C

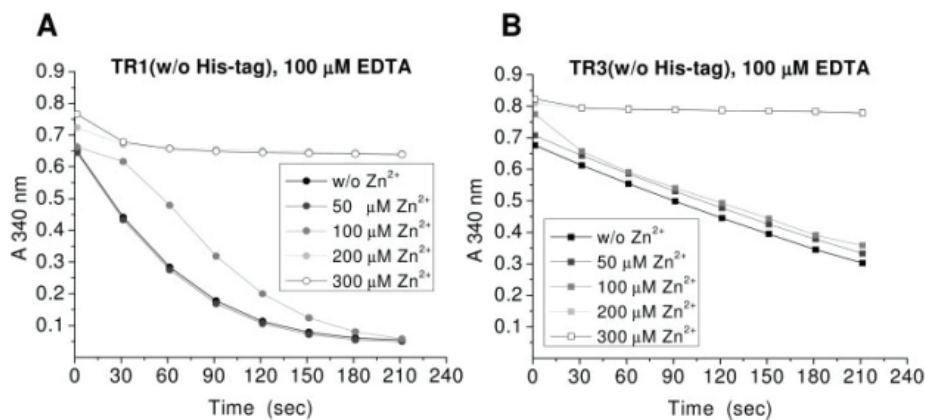


FIGURE 6. Effect of Zn^{2+} ions on the activities of TR1 and TR3 lacking His tags. His tags were removed from the recombinant proteins by thrombin cleavage and affinity isolation, followed by activity assays as shown in Figures 4 and 5. A, TR1 activity; B, TR3 activity.

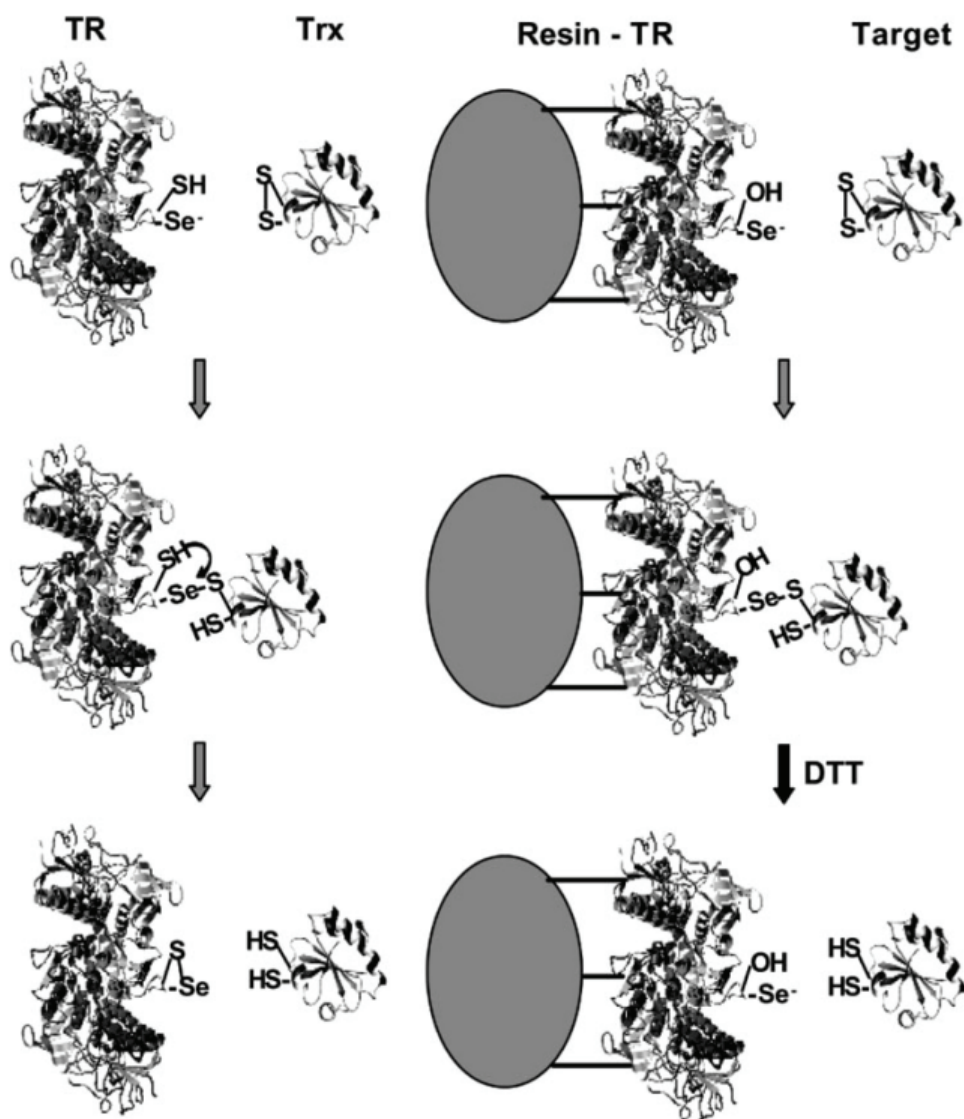


FIGURE 7. Schematic representation of the mechanism-based method for identification of TR3 targets. Various recombinant TR3 forms differing in C-terminal tetrapeptide sequences (see Table 2) were immobilized to prepare the corresponding affinity resins. The immobilized enzymes were reduced with NADPH; cell lysates were applied; resins were washed; and the proteins specifically bound to the resins were eluted with a DTT-containing buffer. *Left panel*, putative mechanism of Trx reduction by TR, in which the reduced selenolthiol group in TR provides, in a two-step process, reducing equivalents to the active-site disulfide in Trx; *right panel*, mechanism-based procedure for identification of TR targets. An SU mutant of an immobilized TR allows trapping of the target via a selenenylsulfide bond. Subsequent addition of DTT elutes the target, which is then subjected to a tandem mass spectrometry procedure for sequencing and protein identification.

resins, whereas the majority of Trx1 was trapped. A second band migrating above the Trx2 band was also detected in two samples. The identity of this band is not known.

Trx Binding Preferences of TR3—The target search experiments suggested that Trx1 may bind TR3 better compared with Trx2, even if it is present in only trace amounts in the mitochondrial fraction. To comparatively analyze mTR3-Trx1 and mTR3-Trx2 interactions, we used recombinant rTrx2 lacking the signal peptide. To test the possibility that Trx2 was blocked from interacting with TR3 due to binding to an unknown protein in the mitochondrial lysate, we added recombinant rTrx2 to the rat liver mitochondrial fraction and applied it to the mTR3 affinity columns. The eluted samples were subjected to Western blotting, and proteins were visualized with anti-Trx1 and anti-His tag monoclonal antibodies to detect His tag-containing recombinant Trx2. Interestingly, even when Trx2 was in excess, TR3 only weakly interacted with this protein, whereas Trx1 was dramatically enriched from essentially undetectable levels (Figure 11). Comparison of the detected Trx bands in the initial sample and eluted fractions revealed enrichment of endogenous Trx1 in the mitochondrial fraction on TR3 columns, but not of Trx2. These data further suggest that reduced TR3 interacts with Trx1 more effectively than with Trx2 *in vitro*.

Discussion

Human, mouse, and rat TR3 genes are similarly organized, and each is characterized by alternative first exon splicing. We have characterized three TR3 isoforms that differ in their N-terminal sequences in these organisms. The previously characterized mitochondrial isoform (TR3a) appears to be a predominant TR3 form in mammals. Two other isoforms (TR3b and TR3c) do not have signal peptides and localize to the cytosol. Although the functions of these two alternative isoforms are unclear, their location outside of mitochondria implies that TR3 may be able to act on substrates other than Trx2. Indeed, we identified cytosolic Trx1 as the major target of TR3. During the preparation of this manuscript, an additional alternative splicing form of TR3 mRNA was identified (32), which has a 3-bp deletion in the coding region and insertion of 1228 bp in the 3'-untranslated region between the stop codon and the SECIS element. These and the previous studies provide further evidence for the complexity of TR3 expression and regulation.

To examine in detail the catalytic properties of TR3, we prepared a recombinant version of this protein in *E. coli*, and in parallel, we also prepared and characterized TR1. Both proteins were expressed as selenoproteins as well as in the form of various mutants that dif-

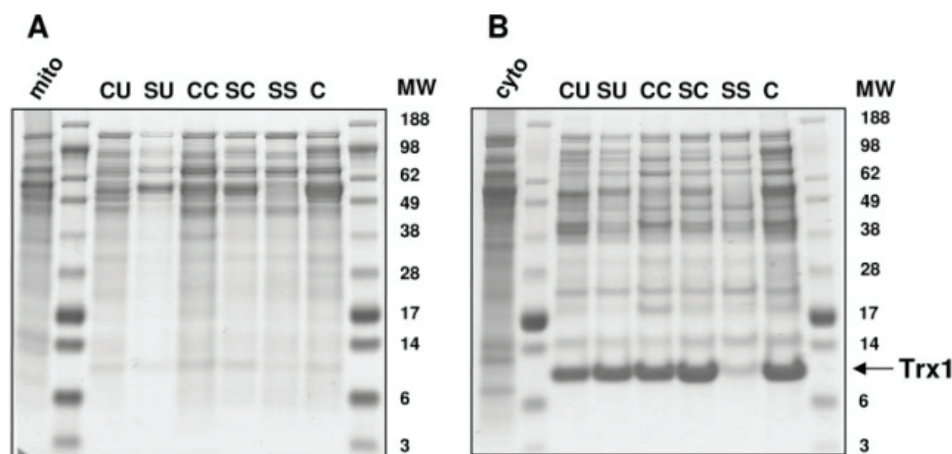


FIGURE 8. Identification of TR3 target proteins. Rat liver mitochondrial and cytosolic fractions were incubated with different mTR3-immobilized resins and washed, and bound proteins were eluted with DTT. The eluted proteins were analyzed by SDS-PAGE, and Coomassie Blue staining was used for visualization. CU, SU, etc., indicate the immobilized forms of TR3 (as in Table 2). The molecular masses of the protein standards are indicated in kilodaltons. *A*, analysis of rat liver mitochondrial (*mito*) lysate; *B*, analysis of rat liver cytosolic (*cyto*) lysate. The arrow indicates the position of Trx1.

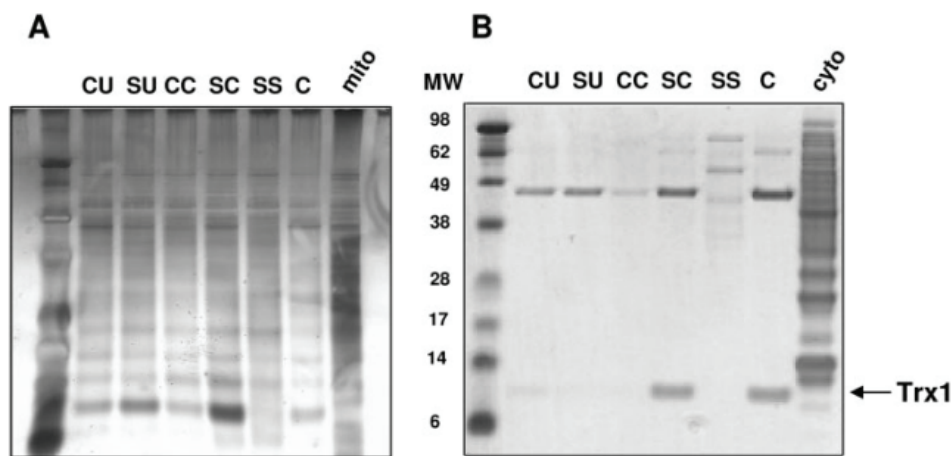


FIGURE 9. Identification of Trx1 as a major target of TR3. Rat liver mitochondrial and cytosolic fractions were incubated with different TR3-immobilized resins. Bound proteins were eluted with DTT and separated by SDS-PAGE. CU, SU, etc., indicate immobilized proteins (Table 2). Extensive washing procedures were applied as described under "Experimental Procedures." The molecular masses of the protein standards are indicated in kilodaltons. *A*, rat liver mitochondrial (*mito*) fraction. Silver staining is shown. *B*, rat liver cytosolic (*cyto*) fraction. The gel was stained with Coomassie Blue. The arrow indicates the position of Trx1.

ferred in their C-terminal sequences. Analysis of the selenium content of recombinant proteins verified efficient Sec insertion: ~50% of recombinant TR3 molecules had Sec, whereas the remaining 50% presumably corresponded to the truncated version, in which protein synthesis terminated at the Sec-encoding UGA codon. As in the case of TR1 (21, 22), efficient Sec insertion into TR3 required elevated expression of Sec insertion machinery, including Sec synthase, tRNA^{Sec}, and SelB.

Analysis of the specific activities of TR1 and TR3 revealed that these enzymes are functional and that their kinetic constants approximately correspond to those of native enzymes isolated from animal tissues and cell lines (33, 34). We have determined the kinetic parameters for various TR substrates (Trx from *E. coli*, Trx1, and Trx2) (Table 1), including the first K_m and k_{cat} values for the TR3/Trx2 pair. Although Trx2 has been proposed as a natural substrate of TR3 by analogy to the TR1/Trx1 pair, our data are the first experimental verification of this prediction. However, comparison of the catalytic efficiencies of TR3 for Trx substrates revealed no preference for Trx2. In fact, TR3 and TR1 exhibited approximately equal activities with Trx1, Trx2, or *E. coli* Trx. This finding is consistent with the complex localization pattern of TR3, as well as TR1, in mammalian tissues and cells.

Another important issue examined in our study was inhibition of TRs by divalent ions. Initial research suggested an inhibitory effect of calcium on TR activity in skin cells (25–27). However, which TR isozyme is the most abundant in skin cells and was inhibited in these studies is not known. Subsequently, TR1 was reported to be insensitive to calcium inhibition (28, 35). However, the most recent study found that TR1, but not TR3, is inhibited by Ca²⁺ (36). Thus, the role of calcium in inhibition of TRs remains unresolved.

Our present work demonstrates that the activities of TR3 and TR1 are not influenced by calcium at physiological levels of this metal ion. There are two major differences between our work and the previous studies. First, the previous inhibitory effect was observed on the native TRs prepared from animal tissues. Second, 5,5'-dithiobis(nitrobenzoic acid) was used to assay the TR activity, whereas we used a more specific method for assaying the activities of Sec-containing recombinant TR1 and TR3 (see "Experimental Procedures").

We also examined the effects of other divalent ions and found a strong inhibitory effect of zinc. It is well known that 1–5 mM EDTA is a required component in TR reaction mixtures; however, the reason for this requirement is not known. There are several possible explanations for the role of EDTA or other metal chelators (e.g. EGTA) in activating TRs. First, TR may bind metals during cell disruption. Second, trace amounts of heavy metals present in the buffers could inhibit TR activity during the purification procedure. EDTA was originally used in extraction buffers during isolation of TR1 from animal tissues (33). We did not use EDTA during purification of recombinant TRs, as the intention was to study the effects of metal ions and chelators on TR activities. We found that the minimal concentration of EDTA needed for maximal TR activity was 100 μ M under our experimental conditions. We have further examined the roles Ca²⁺, Zn²⁺, and Co²⁺ ions in TR activities, but only zinc efficiently inhibited TRs. The inhibitory effect of Zn²⁺ could be explained by the natural affinity of the zinc ion for protein thiol groups. The active site of TRs has three thiol and one selenol groups, which could potentially serve as zinc ligands.

To further examine Trx2 as a TR3 substrate and to determine the identity of other TR3 targets, we developed a reaction mechanism-

based procedure illustrated in Figure 7, which could also be generally used for determination of TR substrates. The C-terminal selenolthiol of TRs is thought to directly interact with oxidized Trx substrates in a 2-electron reduction process. We hypothesized that mutation of a TR3 residue that reduces the intermediate TR-Trx disulfide (or selenenylsulfide) bond could stabilize the intermolecular complex, which could then be enriched on affinity columns containing mutant TR3 forms.

This hypothesis was tested by analyzing cytosolic and mitochondrial fractions from rat and mouse livers. Surprisingly, Trx1 was identified as the major target of TR3 in both cytosolic and mitochondrial fractions. The failure of Trx2 to bind TR3 effectively could potentially be due to differences in the redox potentials of Trx1 and Trx2 or to other factors. Recently, the redox potential of Trx2 was reported to be lower (-295 to -330 mV) than that of Trx1 (-230 mV) (37). Thus, in the equilibrium with TR3, most Trx2 molecules may be in the oxidized form and therefore not trapped on the TR3 affinity resins.

Although the structures of TR1 (38), TR3 (39), and Trx2 (40) have been determined, little is known about the specific details of the TR-Trx interaction. Our data on the target identification as well as the TR-Trx interaction experiments revealed that the C-terminal tetrapeptide is indeed the interaction partner of Trx. The mutant enzyme lacking both Cys and Sec in the tetrapeptide failed to interact with the substrates. However, various single mutants were effective in trapping Trx1. Although these data leave open the question of whether Sec or Cys is the attacking residue in the reaction with Trx substrates, it appears that either residue can serve this function if the other is missing.

The finding that the truncated TR3 form lacking the last two residues was most efficient in binding Trx1 pointed to the potential mechanism by which this form contributes to apoptosis (31). Based on the Trx trapping experiments, it is expected that a stable TR3·Trx1 complex (and likely other TR·Trx complexes) would be formed in cells in the presence of truncated TRs, thus stably binding thioredoxins and influencing redox homeostasis.

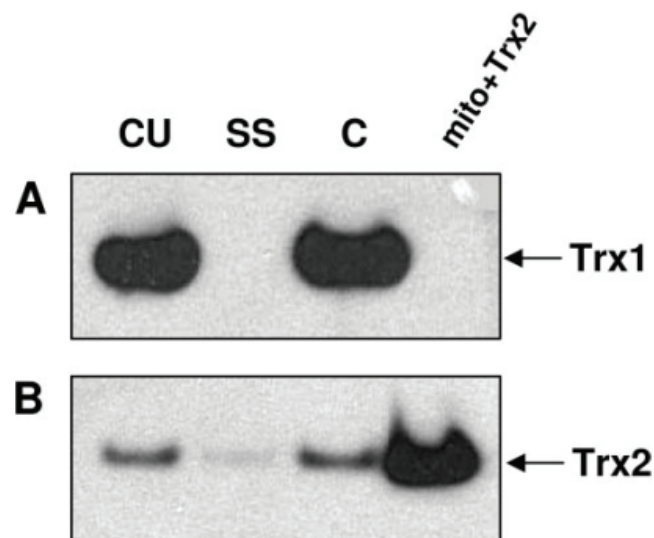


FIGURE 10. Analysis of Trx1 and Trx2 interactions with TR3. Rat and mouse liver mitochondrial and cytosolic fractions were incubated with different mTR3-immobilized resins. Bound proteins were eluted with DTT and separated by SDS-PAGE, followed by Western blotting. Trx1 and Trx2 were detected with specific anti-Trx1 and anti-Trx2 antibodies. *A*, rat liver mitochondrial (*mito*) fraction; *B*, rat liver cytosolic (*cyto*) fraction; *C*, mouse liver mitochondrial fraction; *D*, mouse liver cytosolic fraction; *E*, Coomassie Blue staining of samples showing protein loading of cytosolic and mitochondrial fractions. The positions of Trx1 and Trx2 are indicated by arrows.

Clearly, the substrate trapping approach could be further applied to other TRs. For example, the heterogeneity of TR1 is even more complex than that of TR3 because TR1 exists in at least six isoforms. Likewise, this method can be applied to search for targets of the third mammalian TR known as thioredoxin/glutathione reductase. This protein has been recently implicated in disulfide bond formation during sperm maturation (41).

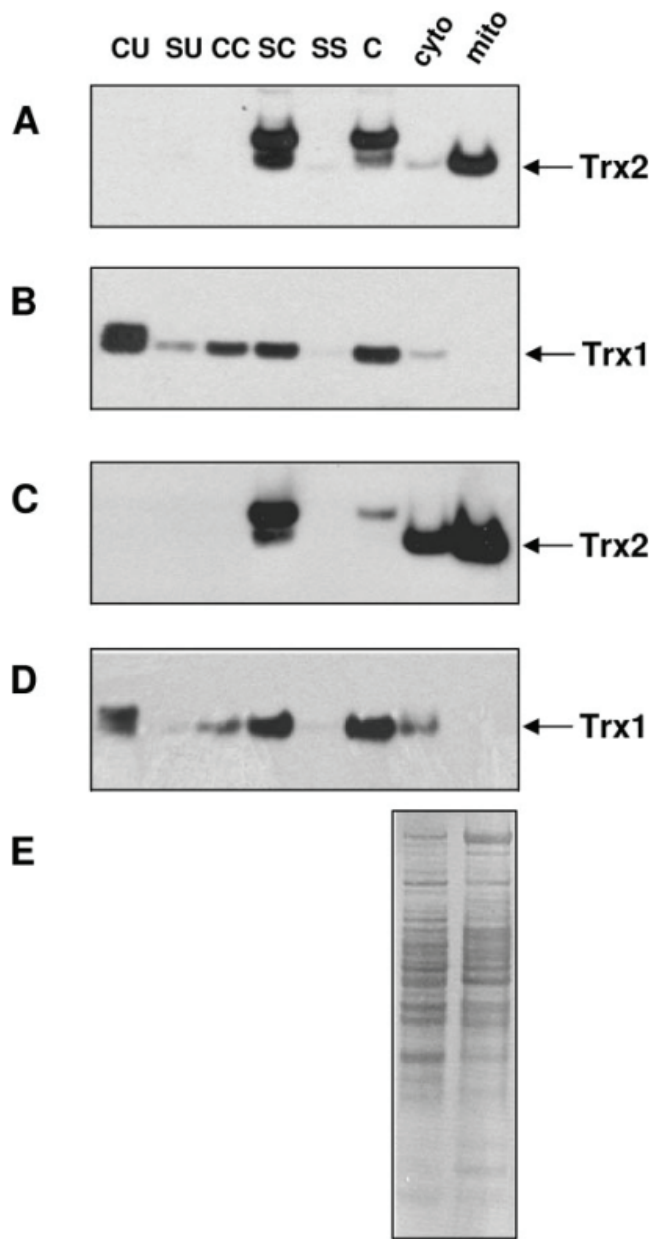


FIGURE 11. Analysis of the interaction between Trx2 and TR3. rTrx2 was added to the rat liver mitochondrial fraction, followed by incubation with mTR3 resins. The bound proteins were separated as described under "Experimental Procedures." *A*, the membrane was stained with anti-hTrx1 antibodies. *B*, the membrane was stained with anti-His tag antibodies. *First lane*, proteins eluted from the CU column; *second lane*, proteins eluted from the SS column; *third lane*, proteins eluted from the C-stop column; *fourth lane*, initial mitochondrial (*mito*) fraction with added rTrx2. The positions of Trx1 and Trx2 are indicated by arrows.

Acknowledgments — We thank Dr. Sergey Novoselov for help with subcellular localization experiments; Dr. Alexey Lobanov for help with sequence analyses; and Drs. Elias Arnér, Antonio Miranda-Vizuete, and Giannis Spyrou for providing expression constructs.

References

1. Holmgren, A. (1985) *Annu. Rev. Biochem.* **54**, 237-271
2. Arnér, E. S., and Holmgren, A. (2000) *Eur. J. Biochem.* **267**, 6102-6109
3. Gromer, S., Urig, S., and Becker, K. (2004) *Med. Res. Rev.* **24**, 40-89
4. Gasdaska, P. Y., Gasdaska, J. R., Cochran, S., and Powis, G. (1995) *FEBS Lett.* **379**, 5-9
5. Gasdaska, P. Y., Berggeren, M. M., Berry, M. J., and Powis, G. (1999) *FEBS Lett.* **442**, 105-111
6. Lee, S.-R., Kim, J.-R., Kwon, K.-S., Yoon, H. W., Levine, R. L., Ginsburg, A., and Rhee, S. G. (1999) *J. Biol. Chem.* **274**, 4722-4734
7. Miranda-Vizuete, A., Damdimopoulos, A. E., and Spyrou, G. (1999) *Biochim. Biophys. Acta* **1447**, 113-118
8. Mustacich, D., and Powis, G. (2000) *Biochem. J.* **346**, 1-8
9. Jakupoglu, C., Przemeczek, G. K., Schneider, M., Moreno, S. G., Mayr, N., Hatzopoulos, A. K., de Angelis, M. H., Wurst, W., Bornkamm, G. W., Brielmeier, M., and Conrad, M. (2005) *Mol. Cell. Biol.* **25**, 1980-1988
10. Conrad, M., Jakupoglu, C., Moreno, S. G., Lippl, S., Banjac, A., Schneider, M., Beck, H., Hatzopoulos, A. K., Just, U., Sinowatz, F., Schmahl, W., Chien, K. R., Wurst, W., Bornkamm, G., and W., Brielmeier, M. (2004) *Mol. Cell. Biol.* **24**, 9414-9423
11. Yamamoto, M., Yang, G., Hong, C., Liu, J., Holle, E., Yu, X., Wagner, T., Vatner, S. F., and Sadoshima, J. (2003) *J. Clin. Investig.* **112**, 1395-1406
12. Nonn, L., Williams, R. R., Erickson, R. P., and Powis G. (2003) *Mol. Cell. Biol.* **23**, 916-922
13. Sun, Q., Zappacosta, F., Factor, V. M., Wirth, P. J., Hatfield, D. L., and Gladyshev, V. N. (2001) *J. Biol. Chem.* **276**, 3106-3114
14. Rundlof, A. K., Janard, M., Miranda-Vizuete, A., and Arnér, E. S. (2004) *Free Radic. Biol. Med.* **36**, 641-656
15. Damdimopoulos, A. E., Miranda-Vizuete, A., Treuter, E., Gustafsson, J. A., and Spyrou, G. (2004) *J. Biol. Chem.* **279**, 38721-38729
16. Su, D., and Gladyshev, V. N. (2004) *Biochemistry* **43**, 12177-12188
17. Lescure, A., Gautheret, D., Carbon, P., and Krol, A. (1999) *J. Biol. Chem.* **274**, 38147-38154
18. Miranda-Vizuete, A., and Spyrou, G. (2002) *Mol. Cells* **13**, 488-492
19. Arnér, E. S., Zhong, L., and Holmgren, A. (1999) *Methods Enzymol.* **300**, 226-239
20. Motohashi, K., Kondoh, A., Stumpp, M. T., and Hisabori, T. (2001) *Proc. Natl. Acad. Sci. U. S. A.* **98**, 11224-11229
21. Arnér, E. S., Sarioglu, H., Lottspeich, F., Holmgren, A., and Bock, A. (1999) *J. Mol. Biol.* **292**, 1003-1016
22. Arnér, E. S. (2002) *Methods Enzymol.* **347**, 226-235
23. Johansson, L., Chen, C., Thorell, J.-O., Fredriksson, A., Stone-Elander, S., Gafvelin, G., and Arnér, E. S. (2004) *Nat. Methods* **1**, 61-66
24. Rengby, O., Johansson, L., Carlson, L. A., Serini, E., Vladimirov-Gardikas, A., Karsnas, P., and Arnér, E. S. (2004) *Appl. Environ. Microbiol.* **70**, 5159-5167
25. Schallreuter, K. U., and Wood, J. M. (1989) *Biochim. Biophys. Acta* **967**, 242-247
Schallreuter, K. U., Pittelkow, M. R., and Wood, J. M. (1989) *Biochem. Biophys. Res. Commun.* **162**, 1311-1316
27. Gitler, C., Zarmi, B., Kalef, E., Meller, R., Zor, U., and Goldman R. (2002) *Biochem. Biophys. Res. Commun.* **290**, 624-628
28. Oblong, J. E., and Powis, G. (1993) *FEBS Lett.* **334**, 1-2
29. Zhong, L., Arnér, E. S., and Holmgren, A. (2000) *Proc. Natl. Acad. Sci. U. S. A.* **97**, 5854-5859
30. Gromer, S., Johansson, L., Bauer, H., Arscott, L. D., Rauch, S., Ballou, D. P., Williams, C. H., Jr., Schirmer, R. H., and Arnér, E. S. (2003) *Proc. Natl. Acad. Sci. U. S. A.* **100**, 12618-12623
31. Anestål, K., and Arnér, E. S. (2003) *J. Biol. Chem.* **278**, 15966-15972
32. Chang, E. Y., Son, S.-K., Ko, H. S., Baek, S.-H., Kim, J. H., and Kim, J.-R. (2005) *Free Radic. Biol. Med.* **39**, 1666-1675
33. Luthman, M., and Holmgren, A. (1982) *Biochemistry* **21**, 6628-6633
34. Zhong, L., and Holmgren, A. (2000) *J. Biol. Chem.* **275**, 18121-18128
35. Valcarce, C., Holmgren, A., and Stenflo, J. (1994) *J. Biol. Chem.* **269**, 26011-26016
36. Rigobello, M. P., Vianello, F., Folda, A., Roman, C., Scutari, G., and Bindoli, A. (2006) *Biochem. Biophys. Res. Commun.* **343**, 873-878
37. Halvey, P. J., Watson, W. H., Hansen, J. M., Go, Y.-M., Samali, A., and Jones, D. P. (2005) *Biochem. J.* **386**, 215-219
38. Sandalova, T., Zhong, L., Lindqvist, Y., Holmgren, A., and Schneider, G. (2001) *Proc. Natl. Acad. Sci. U. S. A.* **98**, 9533-9538
39. Biterova, I. E., Turanov, A. A., Gladyshev, V. N., and Barycki, J. J. (2005) *Proc. Natl. Acad. Sci. U. S. A.* **102**, 15018-15023
40. Smeets, A., Evrard, C., Landtmeters, M., Marchand, C., Knoops, B., and Declercq, J. P. (2005) *Protein Sci.* **14**, 2610-2621
41. Su, D., Novoselov, S. V., Sun, Q. A., Moustafa, M. E., Zhou, Y., Oko, R., Hatfield, D. L., and Gladyshev V. N. (2005) *J. Biol. Chem.* **280**, 26491-26498

Supplementary Data

PCR primers used in cloning and preparation of chimeric gene expression constructs

- 1 mTR3a 1 5'-TATTAAGAAATTCATGGCGGCGATGGTGGCCGG -3'
- 2 mTR3 rew 5'-ATTAATGGGCCCGCCGCAGCAACCAGTCACAG -3'
- 3 mTR3a 5'-CTGACACGCGGGACAAGGGGCGCGGCGAGTGCAGCGGGAGGG-3'
- 4 mTR3a 5'-GGCGCTTCCGGCCGCGGACACGGGCTCTGACACGCGGGACAAG-3'
- 5 mTR3a 5'-ATGTGGGCGGCGCTGCGTGGACCCAGCAGGCGCTTCCGGCCGC-3'
- 6 mTR3a 5'-ATGGCGGCGATGGTGGCCGGGCGAATGTGGGCGGCGCTGCG-3'
- 7 mTR3b 5'-GAGACTGAAATTCATGGAAGGGCAGCAGAGCTTTGATCTCTTG-3'
- 8 mTR3c 5'-CAGAAGGACAGGCCTAAGCACAGGCAGCAGAGCTTTGATCTC-3'
- 9 mTR3c 5'-TACATTGAAATTCATGAGCTGTGGGCAGAAGGACAGGCCTAAG-3'
- 10 mTR3(w/o) 5'-TACATTGAAATTCATGGCGAGTGCAGCGGGAGGCAG -3'
- 11 mTR3 CU f 5'-ATTTATAGCTAGCGCGAGTGCAGCGGGAGGGC-3'
- 12 mTR3 CU 5'-GCAGACCTGCAACCGATGTTAGCCTCAGCAACCAGTCAC-3'
- 13 mTR3 CU r 5'-TAAGAAATTCGCGACCGATTGGTGCAGACCTGCAACCGATG-3'
- 14 mTR3 SU 5'-GCAGACCTGCAACCGATGTTAGCCTCAACTACCAGTCACAG-3'
- 15 mTR3 CS 5'-ACTGCGAAATTCTTAGCCACTGCAACCAGTCACAG-3'
- 16 mTR3 CC 5'-ACGGCGAAATTCTTAGCCGACGACACCATGCACAG-3'
- 17 mTR3 SS 5'-ACGGCGAAATTCTTAGCCACTACTACCAGTCACAGTAGG-3'
- 18 mTR3 C 5'-ACGGCGAAATTCTTAGCAACCAGTCACAGTAGGCTCC-3'